

A. PAWŁOWSKI*, T. CZEPEPE*, J. MORGIEL*, L. GÓRSKI**, W. BALIGA*

PHASE COMPOSITION OF THE PLASMA SPRAYED $\text{Al}_2\text{O}_3\text{-ZrO}_2$ LAYER ONTO METALLIC SUBSTRATE

SKŁAD FAZOWY WARSTWY $\text{Al}_2\text{O}_3\text{-ZrO}_2$ NATRYSKIWANEJ PLAZMOWO NA PODŁOŻE METALICZNE

The results of investigation of $\text{Al}_2\text{O}_3+40\text{wt.}\%\text{ZrO}_2$ oxide layer plasma sprayed on Ni superalloy substrate with NiCrFeAl interlayer have been presented. The coating was subjected to annealing at 1350°C for 15 hours. The oxide layer was examined using scanning (SEM) and transmission (TEM) electron microscopy along with diffraction (SADP) techniques and chemical analysis in microareas (EDX). The X-ray phase analysis of the layer was carried out to observe changes at different distances from the surface. It was found that near the surface up to $100\ \mu\text{m}$ the highest intensity was observed $\text{ZrO}_2\text{-m}$ while $\text{Al}_2\text{O}_3\text{-}\gamma$ phase gave much lower intensity. Near the metallic substrate up to $10\ \mu\text{m}$, an amorphous phase based on Al_2O_3 and rich in ZrO_2 prevailed. During annealing in partially crystallized forming $\text{Al}_2\text{O}_3\text{-}\alpha$ and $\text{ZrO}_2\text{-c}$ phases. The $\text{ZrO}_2\text{-m}$ phase transformed into $\text{ZrO}_2\text{-t}$.

Keywords: $\text{Al}_2\text{O}_3\text{-ZrO}_2$ layers, plasma sprayed

W pracy przedstawiono wyniki badań warstwy tlenkowej o składzie $\text{Al}_2\text{O}_3+40\%$ cięż. ZrO_2 natryskiwanej plazmowo na podłożu z nadstopu niklu z międzywarstwą NiCrFeAl. Złącze poddano następnie wyżarzaniu w 1350°C przez 15 godzin w celu ustabilizowania struktury. Do badań zastosowano metody skaningowej (SEM) i transmisyjnej (TEM) mikroskopii elektronowej wraz z dyfrakcją elektronową i analizą składu w mikroobszarach techniką EDX. Przeprowadzono także rentgenowską analizę fazową warstwy tlenkowej na różnych odległościach od powierzchni. Stwierdzono, iż w jej sąsiedztwie tj. do $100\ \mu\text{m}$ największą intensywność linii obserwuje się dla faz $\text{ZrO}_2\text{-m}$ oraz wyraźnie niższą dla faz $\text{Al}_2\text{O}_3\text{-}\gamma$. W pobliżu metalicznego podłoża tj. do $10\ \mu\text{m}$ dominuje faza amorficzna na bazie Al_2O_3 bogata w ZrO_2 , która ulega w wyniku wyżarzania, częściowej krystalizacji z tworzeniem faz $\text{Al}_2\text{O}_3\text{-}\alpha$ oraz $\text{ZrO}_2\text{-c}$. Faza $\text{ZrO}_2\text{-m}$ przekształca się w $\text{ZrO}_2\text{-t}$.

1. Introduction

The ceramic layers plasma sprayed onto metallic substrate work as typical thermal barriers in engines and turbine blades. Plasma sprayed ceramics based on ZrO_2 has been the material of extremely high isolation properties [1]. Nearly as good are the $\text{Al}_2\text{O}_3+\text{TiO}_2$ or $\text{Al}_2\text{O}_3+\text{ZrO}_2$ layers which are also cheaper [3].

As it follows from the up date research on microstructure of coverings, it is typical of them to contain flattened grains close to the metallic substrate as a result of plasma spraying. On the other hand, fast heat outflow is responsible for the formation of columnar crystals, which is typical for the $\text{ZrO}_2+\text{TiO}_2$ ceramics. The grains which solidify last become almost spherical and are strongly segregated [2].

The $\text{Al}_2\text{O}_3\text{-ZrO}_2$ layers frequently reveal sublayer form. The examinations on transmission electron mi-

croscopy (TEM) using electron diffraction techniques (SADP) showed the presence of an amorphous phase based on Al oxide enriched in Ti or Zr ones [2, 4]. Apler [5] reported the existence of eutectics containing 42.6wt% ZrO_2 in the $\text{Al}_2\text{O}_3\text{-ZrO}_2$ equilibrium system. He also found that there is little solubility on the Al oxide side and quite high up to 7wt% Al_2O_3 on the ZrO_2 side. The earlier studies of the phase composition on the $\text{Al}_2\text{O}_3+40\text{wt.}\%\ \text{ZrO}_2$ surfaces sprayed and annealed at 1200°C using techniques (XRD) diffraction showed the presence of ZrO_2 with monoclinic and cubic symmetry as well as hexagonal $\text{Al}_2\text{O}_3\text{-}\alpha$ phases [6].

The aim of this work to study the phase composition of the $\text{Al}_2\text{O}_3+40\text{wt}\%\text{ZrO}_2$ ceramics plasma sprayed on the Ni superalloy substrate at various distances from the surface as well as the identification of phases based on the examination of the composition in microareas and electron diffraction techniques.

* INSTITUTE OF METALLURGY AND MATERIALS SCIENCE, POLISH ACADEMY OF SCIENCES, 30-059 KRAKÓW, 25 REYMONTA STR., POLAND

** INSTITUTE OF ATOMIC ENERGY, 05-400 ŚWIERK-OTWOCK, POLAND

2. Experimental procedure

The plasma spraying with a ceramic powder melted in a electric arch in plasma hydrogen and argon atmosphere was carried out in PN-120 plasmathrone in Świerk-Poland according to parameters given in the work of Górski [6].

The ceramic material was introduced as Al_2O_3 corundum in the amount of 60% and ZrO_2 in the amount of 40% with grains 10-80 μm in size. It took several milliseconds to reach temperature about 10^4 K, while the cooling rate of the layer obtained on the metallic substrate, was assessed to be 10^5 - 10^6 K/s. The stainless steel was the substrate, which was plasma sprayed with a Ni-20 Cr-5 Fe-2 interlayer, to improve the adherence of the ceramic cover. The thickness of the ceramic layer obtained was about 200 μm . The coating was subjected to annealing at 1350°C for 15 hs, in order to stabilize the structure and improve the adherence of the layer to the substrate.

The X-ray phase analysis of the layer, of which subsequent layers of about 50 μm had been removed, was carried out on Philips PW 1710 diffractometer using CuK_α radiation. The analyses of grain morphology and chosen areas of the layer as well as the composition of the ceramic and transition layer at cross-section were realized using a scanning electron microscope SEM Philips XL 30 equipped with EDX LINK device and a Philips CM20 Twin transmission microscope. Thin foils for TEM were produced with two techniques: thinning with the Focused Ion Beam (FIB) method using a Ga beam in a Quanta 3D microscope, for the case of areas close to the substrate and using conventional ion thinning technique for studying the full cross-section of the ceramic layer. The local chemical analysis of composition was carried out on an EDAX Phoenix device using the 10 nm wide beam.

3. Results

3.1. SEM microstructure and chemical EDX analyses

The observations of Al_2O_3 +40wt% ZrO_2 ceramic cover using SEM technique confirmed its layer morphology in which a number of sublayers are frequently separated with voids (Fig. 1a). Near the Ni-20Cr-5Fe-2Al interlayer, 10-30 μm from the substrate the EDX measurements detected the ZrO_2 rich, three component ZrAlO_x phase as 10-30 μm inlands of eutectic composition ($E = 42.6\%\text{ZrO}_2$) which is shown in Fig. 1b. Differences in composition E, marked with flat lines, may suggest gradients in distribution of Al. and Zr in the areas investigated. Inside the ceramic a step like change of Ni

and Fe content on the boundary with the substrate was observed, which may indicate their diffusion out of interlayer to the cover layer annealing. Subsequent sublayers contained ZrO_2 and Al_2O_3 phases. The size and number of Al_2O_3 grains increase at 100 μm from the surface.

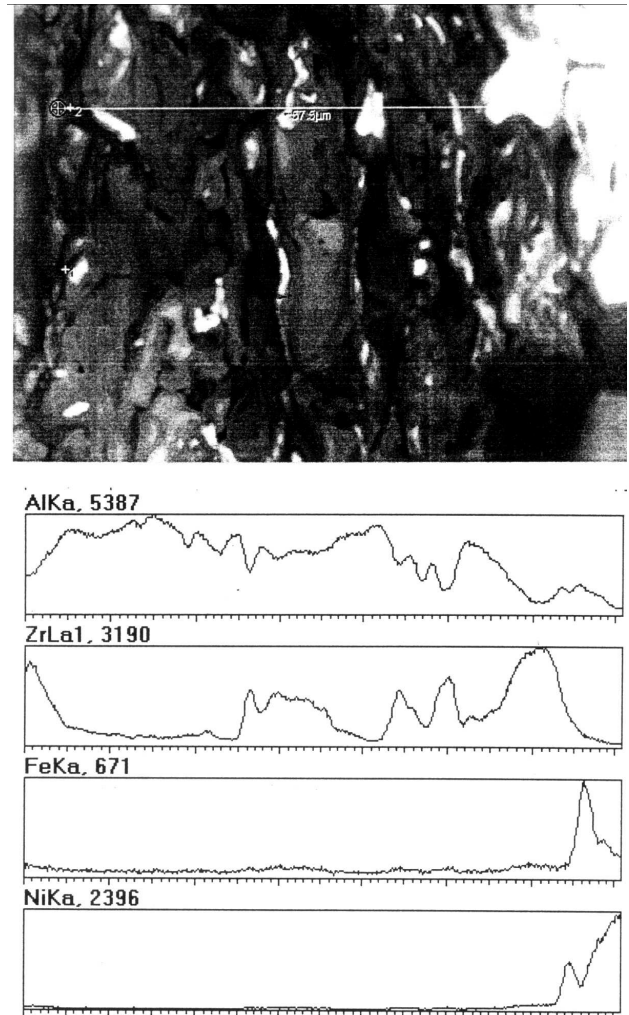


Fig. 1. a) SEM microstructure of the plasma sprayed Al_2O_3 +40wt% ZrO_2 ceramic layer after annealing at 1350°C ; b) The analysis of composition along the line marked in a)

3.2. The X-ray phase analysis

The X-ray phase analysis carried out at various distances from the surface showed that the resulting from the solidification phases like ZrO_2 -m (monoclinic) as well as supersaturated Al_2O_3 - γ phase (cubic) gave the biggest intensity near the layer surface up to 100 μm (Fig. 2a) The intensities of ZrO_2 -t (tetragonal) and ZrO_2 -c (cubic) coming from the solidification of the supersaturated eutectic E phase (Fig. 2b) after annealing at 1350°C had the lowest intensity at about 50 μm from the surface, while the intensity of Al_2O_3 - α (hexagonal), which appeared at annealing was the highest at the surface layer. The phase composition has been shown in the phase system in Fig. 3.

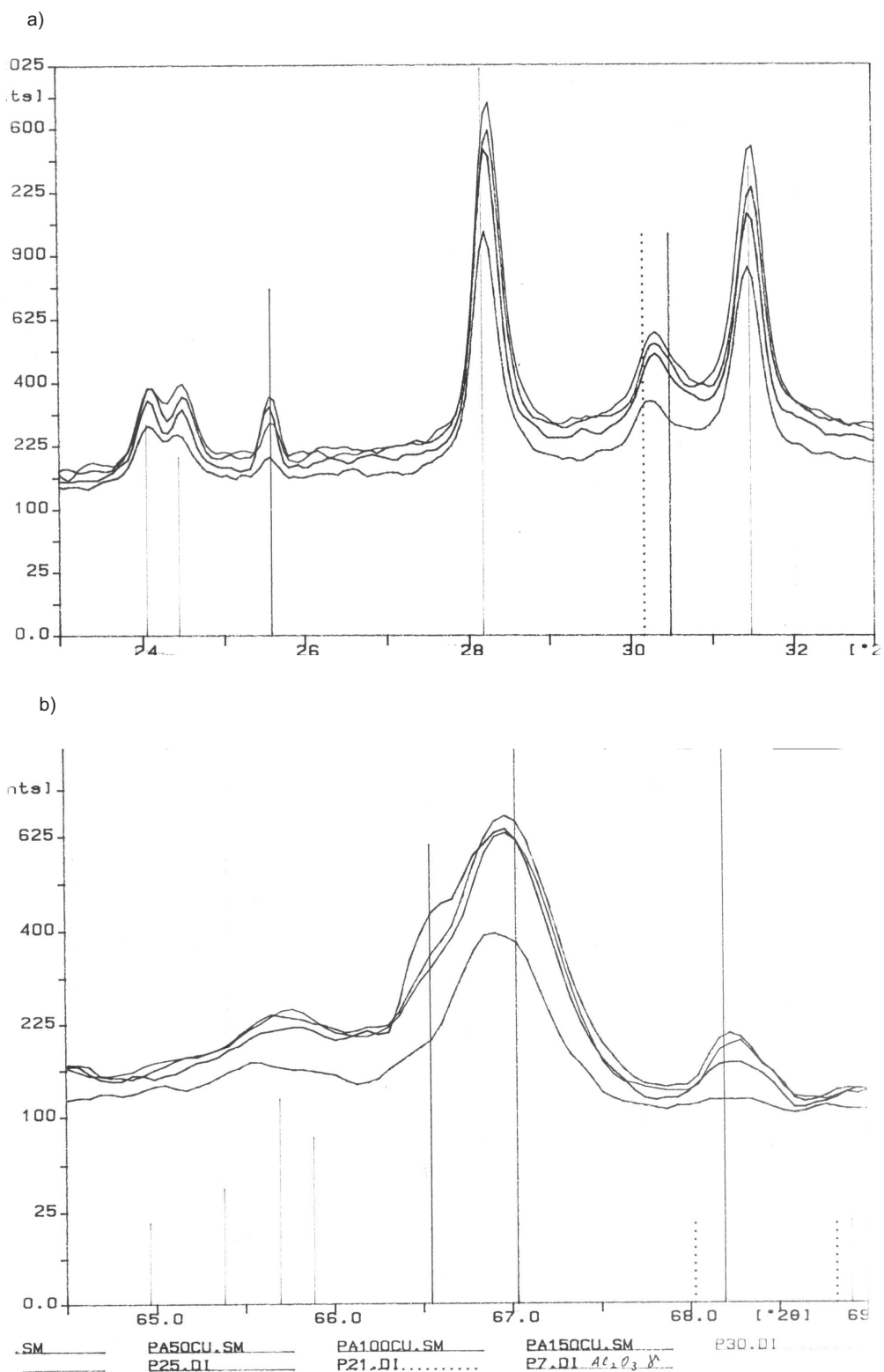


Fig. 2. a) XRD phase analysis of the plasma sprayed $\text{Al}_2\text{O}_3+40\text{wt}\%\text{ZrO}_2$, range $24-33^\circ$, (1)-the surface of the sample, (2)-50 μm , (3)-100 μm , (4)-150 μm below the surface; b) XRD phase analysis of the plasma sprayed $\text{Al}_2\text{O}_3+40\text{wt}\%\text{ZrO}_2$, range $64-69^\circ$, (1)-the surface of the sample, (2)-50 μm , (3)-100 μm , (4)-150 μm below the surface

3.3. TEM microstructure and EDX analysis

$\text{Al}_2\text{O}_3\text{-ZrO}_2$ (concl.)

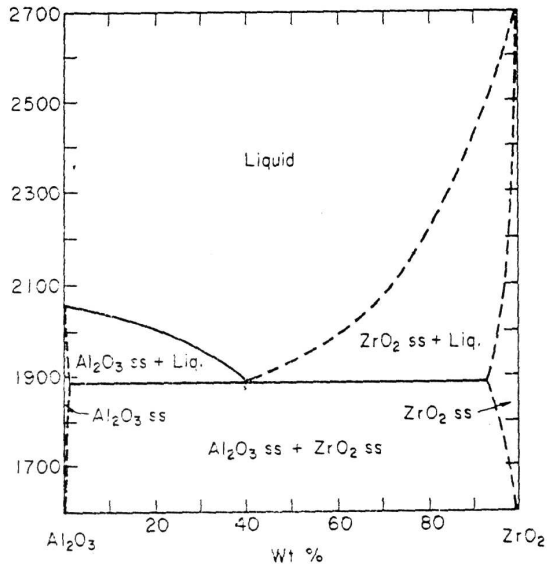


Fig. 3. Phase equilibrium diagram of $\text{Al}_2\text{O}_3\text{-ZrO}_2$ [2]

The observations using transmission microscopy were carried out on thin foils prepared in two ways. First one consisted in thinning with a Ga beam of high energy (FIB) which was extremely suitable in studying microstructure and analysis of composition in microareas close to the substrate. TEM microstructure of the $\text{Al}_2\text{O}_3\text{+40wt\% ZrO}_2$ ceramics layer obtained with this technique are presented in Fig. 4 a,b and 5 a,e. A $\text{ZrO}_2\text{-m}$ particle in Al-rich phase is shown in Fig. 4a. A part of metallic interlayer can be seen in the right lower corner of Fig. 4b. A general view of the microstructure close to the substrate is shown in Fig. 5a, in which an area of the amorphous phase together with fine crystalline lamellas resulting from its partial crystallization may be observed. Fig. 5b presents further view of the structure towards the substrate (right lower corner), in which amorphous phase around the $\text{ZrO}_2\text{-m}$ particle together with a corresponding diffraction pattern may be seen. Based on the EDX analysis it seems that the amorphous phase has the eutectic composition (Fig. 4b). In that area also Al_2O_3 and ZrO_2 particles appear, which was confirmed by the composition analysis shown in Fig. 5 d,e,f. Such analysis due to special technique of producing foils (FIB) is very exact.

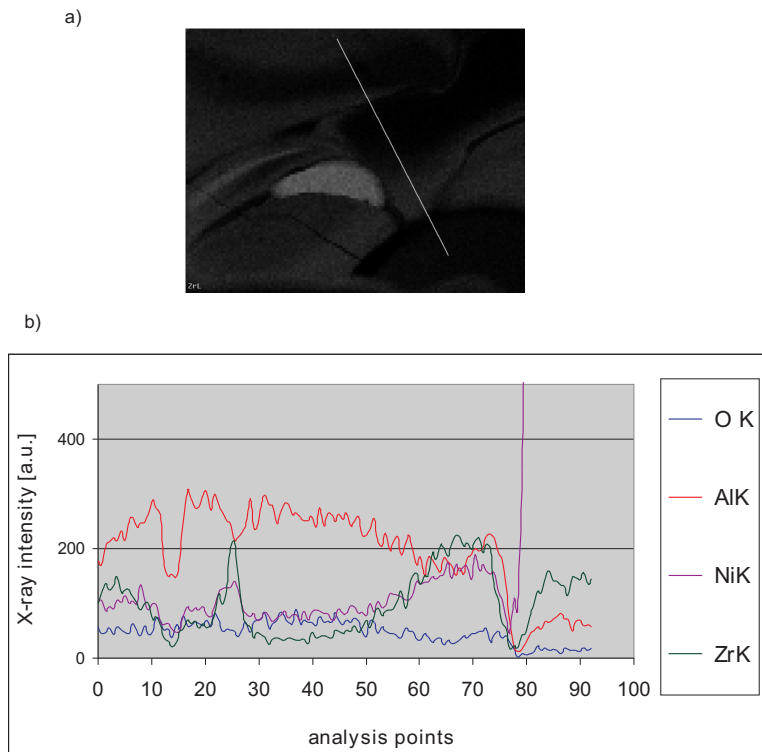


Fig. 4. TEM microstructure and line analysis of composition EDX; (a) microstructure of the $\text{Al}_2\text{O}_3\text{-ZrO}_2$ ceramic layer close to the substrate, (b) analysis of composition along the line marked in Fig. 1a

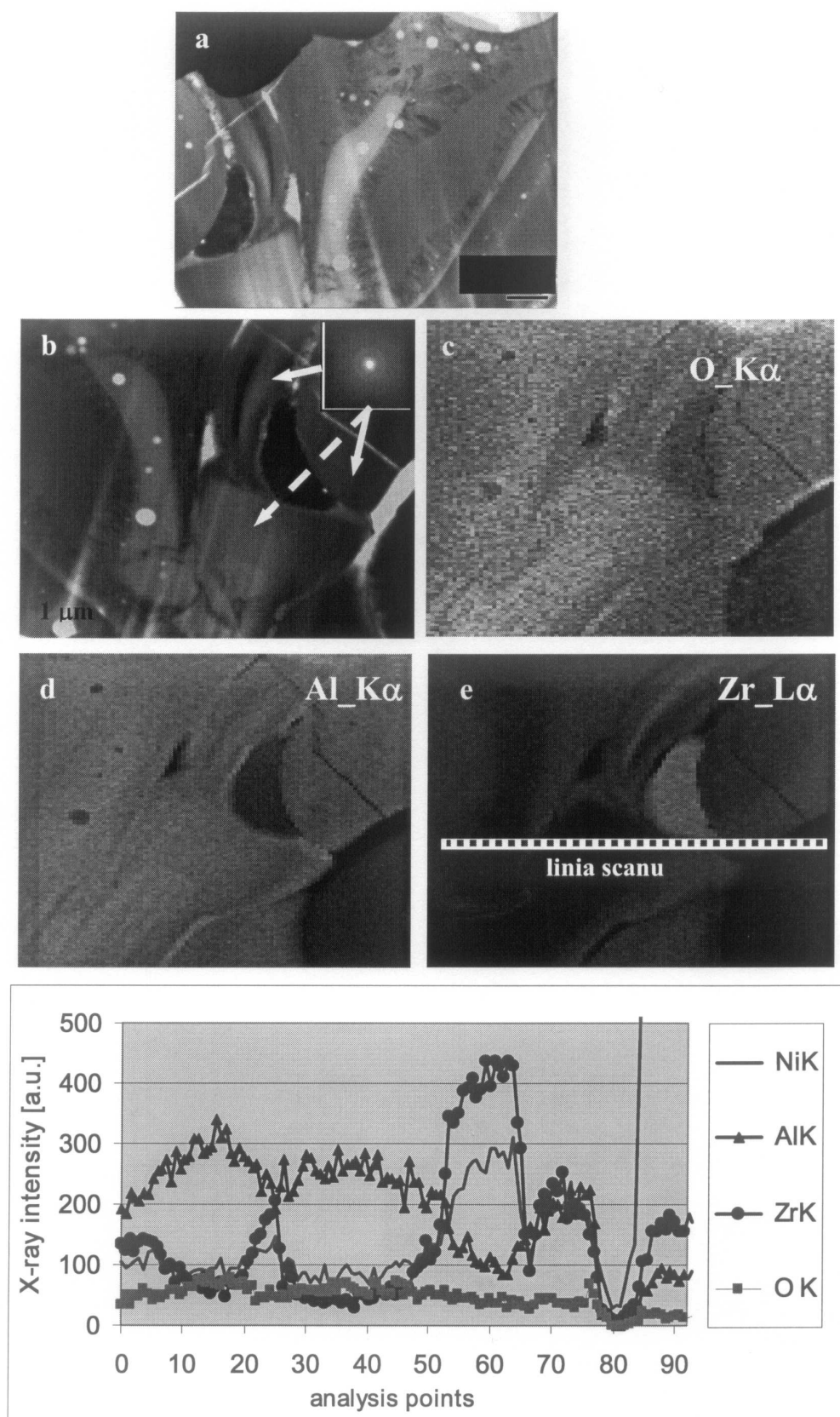


Fig. 5. TEM microstructure (a,b); maps of distribution of elements (c,d,e) and analysis of composition (f)

The thin foil of the ceramic layer produced using convectional thinning helped to obtain a general view of the whole crosssection (Fig. 6). Its morphology consists of sublayers marked A, B, C in the direction from the surface my be seen, in which single columnar crystals are present. The details of the microstructure at the surface of the ceramic layer from Fig. 6 are visible in Fig. 7a. The dark sublayer contains the $\text{ZrO}_2\text{-c}$ [001] phase while the area marked with an arrow in made of the $\text{Al}_2\text{O}_3\text{-}\gamma$ [-114] phase (Fig. 7b,c). Between the A and B sublayers, a fine crystalline transition sublayer 150 nm wide to be seen (Fig. 8a-c).

The EDX point analyses of composition confirmed that the amorphous areas visible in Fig. 9a was an $\text{Al}_{50}\text{O}_{43}\text{Si}_5$ phase, while the columnar crystal had $\text{Zr}_{43}\text{O}_{45}\text{Al}_6$ composition. The solution of the corresponding diffraction pattern confirmed it was $\text{ZrO}_2\text{-c}$ (Fig. 9d). The maps of distribution of Zr, Al, and O taken from the area, presented in Fig. 10 a,b,c also followed the results of the point analyses. It seems as it the Si addition, as well as rapid cooling of the close to surface layer, slowed down the process of crystallization even at annealing at 1350°C , giving as a result a partially stabilized amorphous E phase.

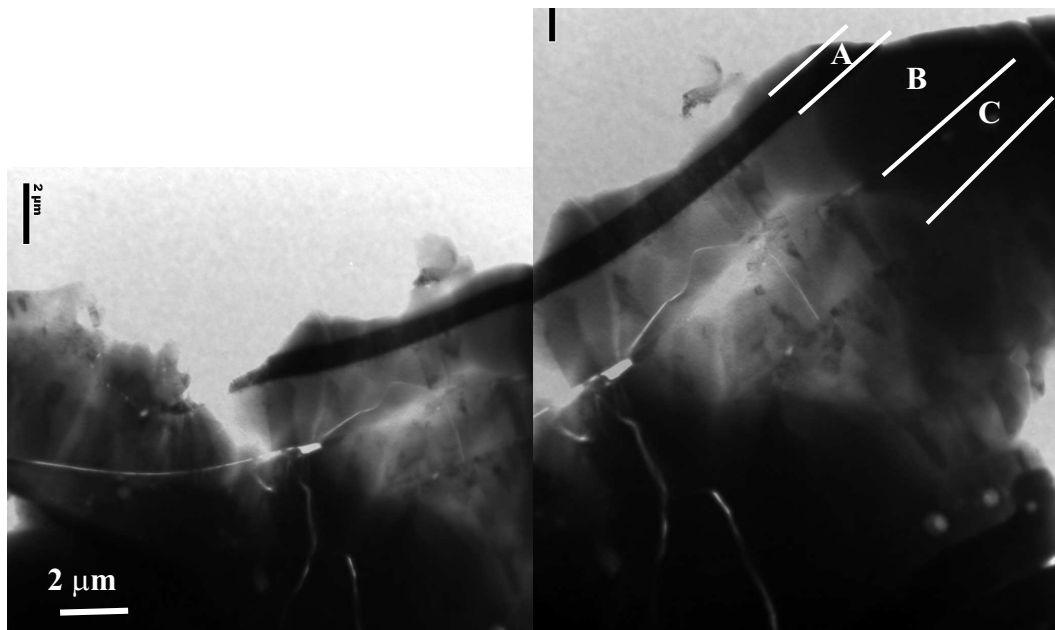


Fig. 6. TEM microstructure, sublayer morphology of the ceramic cover close to the surface

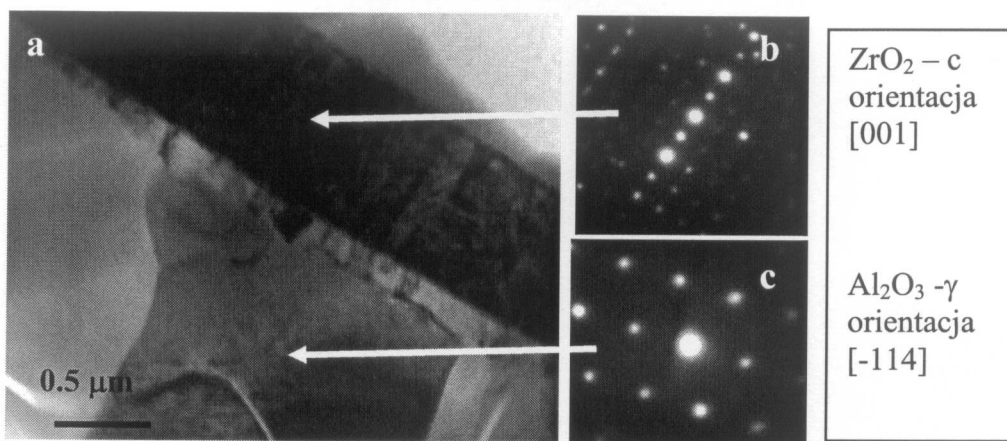


Fig. 7. TEM microstructure close to the A sublayer, a) with electron diffraction patterns from this area, (b, c)

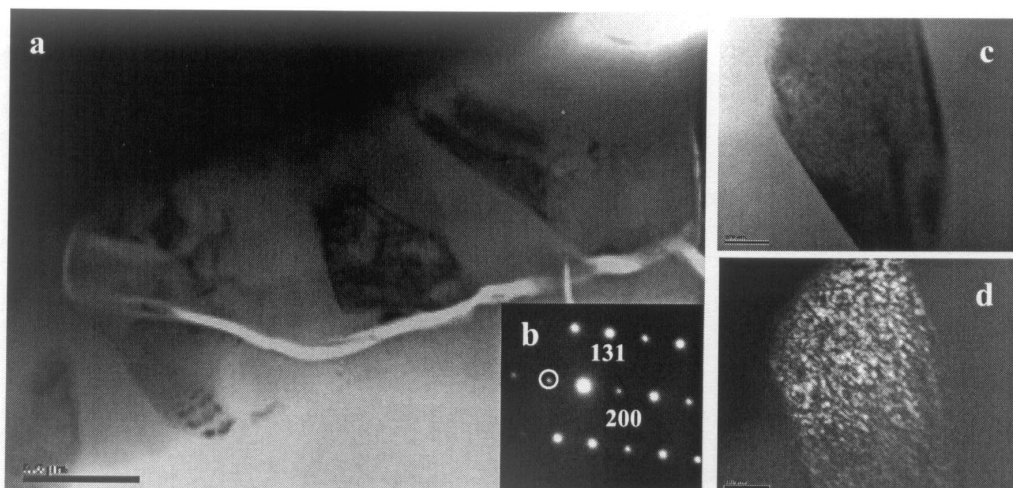


Fig. 8. TEM microstructure of the ceramic cover on the boundary with the metallic substrate, (a)- SAED taken from a single $\text{Al}_2\text{O}_3\text{-}\alpha$ along [103] direction, (b)-bright image (BF), (c)- and dark field image (DF) taken at the reflex marked in the SAED

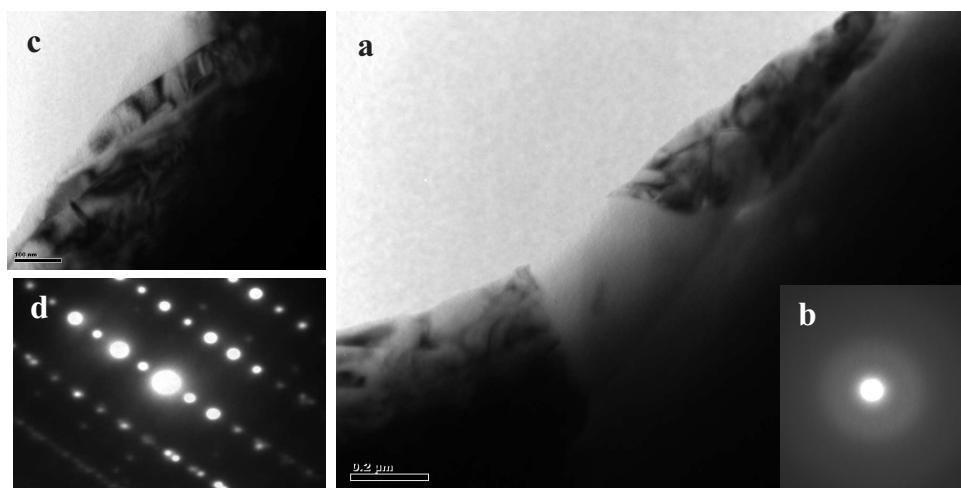


Fig. 9. TEM microstructure of the amorphous phase among $\text{ZrO}_2\text{-c}$ crystals, (a)-SAED from the amorphous area, (b)- TEM image of the ZrO_2 area, (c)- SAED of the crystalline $\text{ZrO}_2\text{-c}$ phase taken along [012] direction

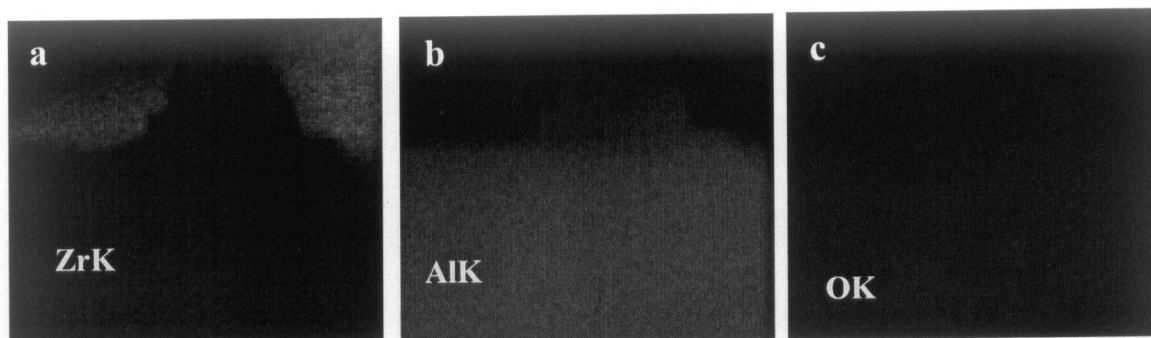


Fig. 10. Maps of distribution of Zr, Al and O in area show in Fig. 9a

4. Discussion and conclusions

The examined ceramic cover of $\text{Al}_2\text{O}_3+40\text{wt}\%\text{ZrO}_2$ composition sprayed on a Ni superalloy substrate containing the interlayer of NiCrFeAl, annealed at 1350°C for 15 hs, was found to form a quite stable phase structure. Transition phases of ZrO_2 -m type with the monoclinic symmetry as well as cubic Al_2O_3 - γ ones, which appeared at rapid cooling after plasma spraying, transformed into stable at lower temperatures ZrO_2 -t and ZrO_2 -c and hexagonal Al_2O_3 - α phases. These observations were confirmed by Górski [6] in measurements with X-ray technique, but the amorphous, supercooled, eutectic E phase, which partially crystallized in the form of lamellar colonies around the amorphous phase, was found for the first time to appear during annealing. The amorphous phase of eutectic composition was reported to exist in the Al_2O_3 - TiO_2 ceramics by the authors of this work in paper [2]. Alternative lamellas of either ZrO_2 -c or ZrO_2 -t or Al_2O_3 - α resulting from a discontinuous solidification inside the colony were a unique observation in the ceramic of the Al_2O_3 - ZrO_2 type. The morphology of the cover changed at various distances from the surface as the effect of appearance of subsequent sublayers and solidified on the already existing ones. At $10\ \mu\text{m}$ distance from the substrate, the islands of the amorphous phase as well as high temperature Al_2O_3 - γ phase and also the ZrO_2 -m one due to quick solidification of the air cooled substrate were observed. The farther from the substrate the slower was the cooling rate causing widening of sublayers of alternative Al and Zr oxides. At about $100\ \mu\text{m}$ distance from the substrate that Al oxide in the large equiaxial form started to prevail on the expense of the Zr oxides. At the surface, the layer morphology of the cover could be no longer observed. The annealing at 1350°C did not bring about the change in the form of grains, but only partial crystallization of the amorphous phase as well as allotropic transitions of Al and Zr oxides. These transitions were responsible for the small amount of microcracks in the cover and thus for its high properties as thermal barrier.

The following conclusions were formulated based on the described investigations:

- The amorphous $\text{Al}_2\text{O}_3+40\text{wt}\%\text{ZrO}_2$ phase of eutectic composition appeared as a result of fast solidification close to the metallic substrate together with the particles of ZrO_2 -m of monoclinic symmetry and [100] orientation as well as the cubic Al_2O_3 - γ phase with [114] orientation.
- A partial crystallization of the amorphous phase took place due to the annealing at 1350°C for 15 hs resulting in the appearance of the ZrO_2 -c phase [1-23] orientation and the hexagonal Al_2O_3 - α one with [013] orientation.
- A sublayer morphology of the covering changed close to the surface into equiaxial grains with a small amount of microcracks.

Acknowledgements

The work was carried out within research IMIM PAS supported by State Committee for Scientific in cooperation with IEA Świerk-Poland.

REFERENCES

- [1] G. Cevalles, *Ber Dent. Keram. Ges.* **45** [5] 217 (1968).
- [2] A. Pawłowski, T. Czeppe, L. Górski, W. Bali ga, *Archives of Metall and Materials* **50** 719-728 (2005).
- [3] T. Czeppe, A. Pawłowski, L. Górski, W. Bali ga, *Archives of Metall. and Materials* **1,2** 103-109 (2005).
- [4] A. Pawłowski, J. Morgiel, L. Górski, *Konf. Kom. Met. PAN Polska Metalurgia* 803-808 (2006).
- [5] A. M. Apler *Science of Ceramics* **3** 137 (1967), Edited by Steward, Academic Press Inc. Londyn.
- [6] L. Górski, *Applied Crystall.* 447-457 (1998).